P_4 and two O_3 molecules. Unlike the case for oxo-bridged P_4O_x molecules, which increased on sample annealing, the Z absorptions decreased on annealing. A relatively high yield of the Z species was also observed after full-arc photolysis of matrices obtained by codeposition of discharged P_4 and Ar/O_3 mixtures.[8] The frequencies of species Z are presented in Table III and compared with the frequencies of the $ClPO_2$, $HOPO_2$, and $OPOPO_2$ molecules.

The two Z bands observed at 1411.3 and 1161.4 cm^{-1} in the -PO stretching region can be assigned with confidence to antisymmetric and symmetric stretching vibrations of a $-PO_2$ group. Their frequencies and $^{16}O/^{18}O$ isotopic ratios (1.02852 and 1.03975) are close to the frequencies and isotopic ratios of $-PO_2$ groups in the $HOPO_2$, $ClPO_2$, and $OPOPO_2$ molecules (see Table III). The 1411.3-cm^{-1} band was split into a triplet at 1410, 1387, and 1371 cm^{-1}, and the 1161 cm^{-1} band produced a triplet at 1160, 1142, and 1118 cm^{-1}, which show two equivalent oxygen atoms in this $-PO_2$ substituent.

The remaining bands for species Z provide further characterization. The 1260.2-cm^{-1} band (isotopic ratio 1.0376) is appropriate for a terminal -PO fundamental. The 592.2-cm^{-1} band (ratio 1.0384) is in the region of symmetric POP vibrations,[1,2] and although the ratio is a little higher than expected for a pure mode, slight mixing with other vibrations can account for the observed ratio. An associated antisymmetric POP stretching mode could easily be obscured by the strong series of absorptions between 856 and 952 cm^{-1}. As Table III shows, the three lower frequency fundamentals are appropriate for bending, waging, and deformation modes of a $-PO_2$ substituent.

The above information is consistent with a $OPOPO_2$ species. Ab initio calculations by Lohr show that the oxo-bridged structures are more stable than P-P-bonded forms.[20] However, two different configurations of $OPOPO_2$ (noted X and Y) have been characterized in $P_2 + O_3$ and $P_2 + O_2$ studies.[8,9] How does species Z produced from $P_4 + 2O_3$ under full-arc irradiation differ from species X and Y? The obvious difference is the presence of a polarizable P_2 molecule in the adjacent matrix site, which may perturb the structure and/or bonding in the probable $OPOPO_2$ species Z, but formation of another rotational $OPOPO_2$ isomer other than those previously observed cannot be excluded. It should be noted that asymmetrical $OPOPO_2$ species Y bands[8] were observed in experiments with a high yield of species Z.

(20) Lohr, L. L., Jr. *J. Phys. Chem.* **1990**, *94*, 1807.

Conclusions

The products formed by matrix photochemical reaction of P_4 with O_3 and in discharged Ar/P_4O_6 mixtures have been studied in solid argon. The major product of red visible photolysis of the P_4--O_3 complex is terminally bonded P_4O, and minor products are oxo-bridged P_4O and a $(P_3)(PO)$ complex. The major products formed on UV photolysis of $Ar/P_4/O_3$ matrices are the oxo-bridged oxides P_4O_x (x = 1-6) and cyclic planar P_4O.

Full-arc photolysis of concentrated $Ar/P_4/O_3$ matrices and low-power discharge of Ar/P_4O_6 mixtures produced a common set of strong absorptions at 941.5, 937.7, and 915.8 cm^{-1} in the region of P-O-P antisymmetric stretching vibrations. These absorptions are assigned to oxo-bridged P_4O_5, P_4O_4, and P_4O_3 oxides, which are formed by stepwise addition of oxygen atoms and/or O_3 molecule to P_4 in O_3 photolysis experiments and in disproportionation reactions of P_4O_6 and O atom elimination from P_4O_6 in discharge experiments. The relatively high yields of P_4O_4 and P_4O_6 on full-arc photolysis in P_4/O_3 experiments suggest that these molecules are formed by photochemical reaction between P_4 and two ozone molecules trapped in the same matrix site.

Acknowledgment. We gratefully acknowledge financial support from NSF Grant CHE 88-20764, preparation of the P_4O_6 sample by J. L. Mills, and the contribution of preliminary discharge experiments with oxygen and red phosphorus by T. R. Burkholder.

Contribution from the Department of Chemistry, University of Florida, Gainesville, Florida 32611

Free Energies of Electron Attachment to Tris(acetylacetonate) and Tris(hexafluoroacetylacetonate) Transition-Metal Complexes in the Gas Phase: Experimental Results and Ligand Field Analysis

Paul Sharpe, John R. Eyler, and David E. Richardson*,†

Received October 2, 1989

Fourier transform ion cyclotron resonance mass spectrometry was used to investigate gas-phase electron-transfer bracketing reactions and charge-transfer equilibria involving parent negative ions formed from a gas-phase mixture of a metal complex and a reference compound. Estimates of the free energies of adiabatic electron attachment at ~350 K (ΔG_a) for tris(acetylacetonate) complexes ($M(acac)_3$, M = Ti, V, Cr, Mn, Fe, Co, Ru) and tris(hexafluoroacetylacetonate) complexes ($M(hfac)_3$, M = Sc, Ti, V, Cr, Mn, Fe, Co, Ga) are reported. The following values of $-\Delta G_a$ (kcal mol^{-1}) for the process $ML_3(g) + e^- = ML_3^-(g)$ were obtained at ~350 K. $M(acac)_3$ complexes: M = Ti, >0; V, 24.9 ± 0.5; Cr, 20 ± 1; Mn, 59 ± 3; Fe, 43.0 ± 0.5; Co, 47 ± 2; Ru, 38.6 ± 0.5. $M(hfac)_3$ complexes: M = Sc, 64 ± 3; Ti, 69 ± 3; V, 73 ± 2; Cr, 67 ± 3; Ga, 60.4 ± 0.5. From the trends in the experimental data, $-\Delta G_a$ values can be estimated for $Mn(hfac)_3$ (~109 kcal mol^{-1}), $Co(hfac)_3$ (~97 kcal mol^{-1}), and $Fe(hfac)_3$ (~93 kcal mol^{-1}). The trends in energies of electron attachment for the acac complexes are analyzed in terms of ligand field theory. Although the ligand field model provides some insight into the general trends in the thermodynamics of electron capture, the details of the trends in the experimental values of ΔG_a are not modeled effectively.

The thermodynamics of redox processes involving solvated reactants and products are available from electrode potentials, which are related to the free energy change accompanying electron attachment to electroactive species in solution. The trends in electrode potentials for various metal/ligand combinations have typically been treated in a phenomenological manner, since accurate quantum calculations are difficult and solvation energetics are not readily obtained. The value of an electrode potential for a particular metal complex can be considered to be the result of two separate contributions, i.e., the intrinsic gas-phase energy for electron attachment to the complex and the solvation energies for the oxidized and reduced forms.[1] For a particular one-electron redox couple, the thermodynamics of the redox process in the

† A. P. Sloan Research Fellow, 1988-1990.

(1) Buckingham, D. A.; Sargeson, A. M. In *Chelating Agents and Metal Chelates*; Dwyer, F. P., Mellor, P. D., Eds.; Academic Press: New York, 1964; pp 237-282.

0020-1669/90/1329-2779$02.50/0

absence of solvent can be obtained by determination of the thermodynamics of the gas-phase electron attachment reaction given in eq 1, where n is the overall charge on the oxidized form.

$$ML_x^n(g) + e^- = ML_x^{n-1}(g) \quad (1)$$

Solvation of the molecular species in eq 1 leads directly to the corresponding solution reaction.[1] The free energy change in solution is given by the single (absolute) electrode potential[2] and can be compared directly to the gas-phase value at the same temperature.[3]

Despite the potential for increasing the understanding of electrode potentials of metal complexes, essentially no reliable gas-phase electron attachment data has been obtained for coordination compounds that can also be studied in solution.[4] The volatile first-row transition-metal tris(β-diketonate) complexes[5] are suitable for such a study.

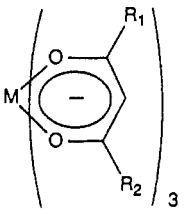

R Group	Ligand	Abbrev.
R_1 and $R_2 = CH_3$	Acetylacetonate	acac
R_1 and $R_2 = CF_3$	Hexafluoroacetylacetonate	hfac

In particular, the tris(acetylacetonate) complexes, abbreviated $M(acac)_3$, and the tris(hexafluoroacetylacetonate) complexes, abbreviated $M(hfac)_3$, have received much attention. These compounds were chosen for this investigation as there have been several reports concerning the stability of their parent negative ions using mass spectrometry[6-8] and describing their electrochemical behavior.[9-13] Both types of experiments involve the formal reduction of the metal from the 3+ to the 2+ oxidation state for the d-open-shell complexes.

Most of the previous studies on the electron attachment to metal-containing compounds have involved volatile metal compounds of weakly polarizable ligands such fluorides and oxides in which the metal has a high formal oxidation state.[14] Neutral compounds of this type (e.g., MF_6) have high electron affinities in the range 3–6 eV, and the physical methods that can be used to determine such high electron affinities often produce disparate results. However, methods for the determination of electron affinities (EA) of polyatomics in the range 0–3 eV are far more reliable (a compilation of physical methods and EA values for many compounds has been recently reviewed by Christopherou[15]). The most prolific method for determining the thermodynamics of electron attachment to neutral molecules has been through investigations of gas-phase charge-transfer equilibria between pairs of organic compounds and their parent negative ions.[16] This work has provided electron attachment free energies (abbreviated $\Delta G_a°$, where the subscript "a" implies electron attachment) for over 200 compounds that span a range of $\Delta G_a°$ values from ca. −0.5 to −3 eV at ~425 K. For many of these compounds the corresponding enthalpy change ($\Delta H_a°$) and entropy change ($\Delta S_a°$) have also been determined. The charge-transfer equilibrium method is easily extended to the series of $M(hfac)_3$ and $M(acac)_3$ metal complexes in this study, as they were often found to have $\Delta G_a°$ values in the same approximate range as the organic reference compounds covered in previous compilations of $\Delta G_a°$ data.

We present here the results of Fourier transform ion cyclotron resonance (FTICR) studies of the thermochemistry of electron attachment to gas-phase $M(acac)_3$ and $M(hfac)_3$ complexes. The free energies of electron attachment to the neutral complexes near room temperature have been estimated by bracketing or through charge-transfer equilibria with organic molecules. The trends in energies of electron attachment to the acac complexes are analyzed by ligand field theory. Thermochemical estimates for metal–ligand bond energies and solvation energies, obtained from the experimental results given here, are presented in a companion article.[17]

Experimental Section

Preparation of $M(hfac)_3$ Complexes. $Cr(hfac)_3$ was purchased from Strem Chemicals Ltd. All other complexes were prepared from the general reaction between the ligand and an anhydrous M(III) chloride, in refluxing carbon tetrachloride.[5] $Ti(hfac)_3$ and $V(hfac)_3$ are oxidized in air and were therefore prepared under an argon atmosphere. In the case of the $Mn(hfac)_3$ and $Co(hfac)_3$ complexes, the alternative methods outlined in ref 18 were most successful. The compounds were purified by repeated sublimations, and their purity was ascertained by mass spectral analysis.

Preparation of $M(acac)_3$ Complexes. All the $M(acac)_3$ complexes were purchased (Strem Chemicals Ltd.) except for $Ti(acac)_3$. The compounds were purified before use by sublimation. $Ti(acac)_3$ was prepared by slowly adding a mixture of acetylacetone and triethylamine to a solution of $TiCl_3$ in ethanol under an argon atmosphere. Purification was effected by repeated recrystallization from degassed ethanol/water mixtures, and the product was sublimed before use.

Organic Compounds. The organic compounds employed in the study were purchased from commercial sources and used without further purification. No extraneous or fragment ions were detected in their negative ion mass spectra.

Electron Attachment Studies. The technique used in this study is similar to that reported previously in ion cyclotron resonance mass spectrometry (ICR)[19-22] and pulsed high-pressure mass spectrometry (PHPMS)[23-28] investigations. Briefly, the time dependence of the pop-

(2) Bard, A. J., Parsons, R., Jordan, J., Eds. *Standard Potentials in Aqueous Solution*; Marcel Dekker: New York, 1985.
(3) The terms *electron affinity* and *adiabatic ionization potential* (or ionization energies) are rather inconvenient to use when thermodynamic relationships between gas-phase and solution redox processes are discussed. Those terms are defined for specific values of n in eq 1 and refer to redox processes at 0 K, but thermodynamics for solution processes are of course defined at $T > 0$ K. Note that in the description of thermochemical cycles connecting electron attachment energetics for gas-phase and solvated species, eq 1 is analogous in form to the standard electrode potential (i.e., $M^n(solv) + e^- = M^{n-1}(solv)$), where the electron is written on the left side. See ref 35 for a complete discussion of thermochemical quantities for gas-phase ion/neutral processes.
(4) Kuge, Y.; Hattori, Y.; Asada, S.; Yamada, S. *Chem. Lett.* **1979**, *3*, 207.
(5) (a) Fackler, J. P. *Prog. Inorg. Chem.* **1966**, *7*, 361. (b) Mehrotra, R. C.; Bohra, R.; Gaur, D. P. *Metal-β-diketonates and Allied Derivatives*; Academic Press, New York, 1978.
(6) Dakternicks, D. R.; Fraser, I. W.; Garnet, J. L.; Gregor, I. K. *Org. Mass Spectrom.* **1979**, *14* (6), 330.
(7) Prescott, S. R.; Campana, J. E.; Risby, T. H. *Anal. Chem.* **1977**, *49* (11), 1501.
(8) Fraser, I. W.; Garnett, J. L.; Gregor, I. K. *J. Chem. Soc., Chem. Commun.* **1974**, 365.
(9) Bond, A. M.; Martin, R. L.; Masters, A. F. *Inorg. Chem.* **1975**, *14*, 1432.
(10) Gritzner, G.; Murauer, H.; Gutmann, V. *J. Electroanal. Chem. Interfacial Electrochem.* **1979**, *101*, 177.
(11) Endo, A.; Watanabe, M.; Hayashi, S.; Shimizu, K.; Sato, G. P. *Bull. Chem. Soc. Jpn.* **1977**, *51*, 800.
(12) Tocher, J. H.; Fackler, J. P. *Inorg. Chim. Acta* **1985**, *102*, 211.
(13) Beaver, B. D.; Hall, L. C.; Lukehart, C. M.; Preston, L. D. *Inorg. Chim. Acta* **1981**, *47*, 25.
(14) Sidorov, L. N. *Russ. Chem. Rev. (Engl. Transl.)* **1982**, *51* (4), 356.
(15) Christodoulides, A. A.; McCorkle, D. L.; Christopherou, L. G. *Electron Molecule Interactions and Their Applications*; Academic: New York, 1984; Vol. 2, pp 423–641.
(16) Kebarle, P.; Chowdhury, S. *Chem. Rev.* **1987**, *87*, 513.
(17) Sharpe, P.; Richardson, D. E. Submitted for publication.
(18) Evans, S.; Hamnet, A.; Orchard, A. F.; Lloyd, D. R. *Faraday Discuss. Chem. Soc.* **1972**, *54*, 227.
(19) McIver, R. T.; Fukuda, E. K. *Lecture Notes in Chemistry*; Hartman, H., Wanzek, K. P., Eds.; Springer: Berlin, 1982; p 164.
(20) Fukuda, E. K.; McIver, R. T. *J. Chem. Phys.* **1982**, *77*, 4942.
(21) Fukuda, E. K.; McIver, R. T. *J. Phys. Chem.* **1983**, *87*, 2993.
(22) Fukuda, E. K.; McIver, R. T. *J. Am. Chem. Soc.* **1985**, *107*, 2291.
(23) Grimsrud, E. P.; Caldwell, G.; Chowdhury, S.; Kebarle, P. *J. Am. Chem. Soc.* **1985**, *107*, 4627.
(24) Chowdhury, S.; Heinis, T.; Grimsrud, E. P.; Kebarle, P. *J. Phys. Chem.* **1986**, *90*, 2747.
(25) Kebarle, P.; Chowdhury, S. *J. Am. Chem. Soc.* **1986**, *108*, 5453.
(26) Chowdhury, S.; Kishi, H.; Dillow, G. W.; Kebarle, P. *Can. J. Chem.* **1989**, *67*, 603.

Table I. Free Energies of Electron Attachment ($\Delta G_a°$) to $M(acac)_3$ and $M(hfac)_3$ Complexes[a]

$Sc(hfac)_3$	-64 ± 3[d]		
$Ti(hfac)_3$	-69 ± 3[d]	$Ti(acac)_3$	<0
$V(hfac)_3$	-73 ± 2[c]	$V(acac)_3$	-24.9 ± 0.5[c]
$Cr(hfac)_3$	-67 ± 3[d]	$Cr(acac)_3$	-20 ± 1[d]
$Mn(hfac)_3$	(-109)[b]	$Mn(acac)_3$	-59 ± 3[d]
$Fe(hfac)_3$	(-93)[b]	$Fe(acac)_3$	-43.0 ± 0.5[c]
$Co(hfac)_3$	(-97)[b]	$Co(acac)_3$	-47 ± 2[d]
$Ga(hfac)$	-60.4 ± 0.5[c]		

[a] All values in kcal mol^{-1}. Temperature = ~350 K. [b] Estimated values obtained by adding 50 kcal mol^{-1} to corresponding value for $M(acac)_3$ complex (see text). [c] Value obtained from measured equilibrium constant. Reference compounds given in Figure 2. [d] Value obtained by bracketing (Scheme I).

ulations of parent negative ions formed from a mixture of known partial pressures of two reactants are monitored as they charge transfer with the neutrals. For the reactions indicated in Scheme I, the free energy involved for electron capture by species B of unknown electron affinity can be bracketed within the lower limit of the known value for A and the upper limit of that for C. When the free energy change is small (≤3 kcal) as in the case of eq 2, the equilibrium populations of the ions can

$$A^- + B \underset{}{\overset{K_{rxn}}{\rightleftharpoons}} A + B^- \qquad (2)$$

be measured. The neutral reactants are in large excess, and their partial pressures do not vary during the reaction. Evaluation of the equilibrium constant K_{rxn} leads to the difference in adiabatic free energy of electron capture for the two reactants ($\Delta G_{rxn}°$). For many of the organic compounds studied, the corresponding entropy changes ($\Delta S_{rxn}°$) and enthalpy changes ($\Delta H_{rxn}°$) have been obtained by following the temperature dependence of the equilibrium.[24,25,27,28] The results have produced ladders of multiple overlapping values of $\Delta G_{rxn}°$, $\Delta H_{rxn}°$, and $\Delta S_{rxn}°$ for pairs of organic reactants such as substituted benzophenones,[22] nitrobenzenes,[20-24,26] quinones,[22,27] and dicarbonyls.[28] The absolute values for electron capture by each compound ($\Delta G_a°$, $\Delta H_a°$, and $\Delta S_a°$ for the reaction $A + e^- = A^-$) are obtained by including an external standard in the ladders for which $\Delta H_a°$ and $\Delta S_a°$ are well established. For example the EA of SO_2 has been accurately determined to be 1.097 ± 0.036[29] and 1.107 ± 0.0008 eV[30] in two independent investigations of the photoelectron spectroscopy of SO_2^-, and SO_2 is the reference compound chosen in the EA investigations of Kebarle.[23-28] The value for ΔS_a for SO_2/SO_2^- was evaluated by the methods of statistical mechanics from structural and spectroscopic data.[24]

Scheme I

$$A^- + B \rightarrow A + B^-$$

$$B^- + C \rightarrow B + C^-$$

Gas-phase charge-transfer reactions of the type outlined in Scheme I and in eq 2 were studied by using a Nicolet FT/MS 1000 Fourier transform ion cyclotron resonance mass spectrometer (FTICR).[31] Most of the organic compounds and the $M(hfac)_3$ complexes were sufficiently volatile to admit into the mass spectrometer through leak valves without heating. Less volatile organics and the $M(acac)_3$ complexes were sublimed off the tip of a solids probe placed ~0.5 m from the ion trap, which was at a temperature of ~350 K. Negative ions were produced from neutrals in the FTICR trap by capture of low-energy electrons (<1 V). Electron capture by the metal complexes was, in most cases, accompanied by varying amounts of fragmentation. Parent ions were selected from these fragments by ion ejection techniques.

To approach collisional thermalization of ions prior to the ion/molecule reaction, FTICR relies on a thermalization period between ionization and detection of product ions. Typical reaction pressures in this study were in the 10^{-6} Torr range, and bath gas such as argon or cyclohexane can be added to reactant mixtures if lower reactant pressures are used.

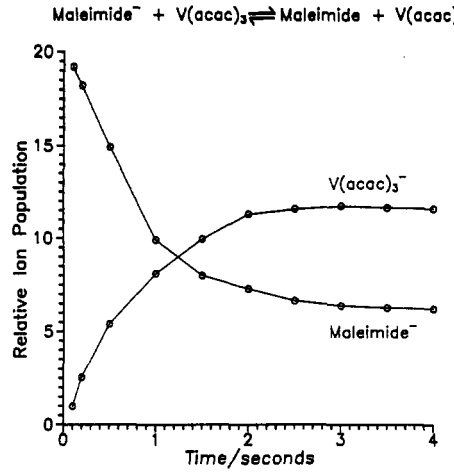

Figure 1. Time dependence of the charge-transfer reaction of maleimide–ions in a background pressure of 1.1×10^{-6} Torr of $V(acac)_3$ and 4.8×10^{-7} Torr of maleimide. Initially all ions except maleimide(−) are ejected from the FTICR reaction cell. A constant ratio of the relative populations of $V(acac)_3^-$ ions maleimide(−) ions is reached after ~4 s.

For bracketing experiments a thermalization period of 1 s was used, providing an average of about ~30 cooling collisions per ion, before subsequent charge-transfer reactions were followed. When a charge-transfer equilibrium was observed, the ion populations were determined by measuring the relative abundance of the two parent ions over suitable time intervals until they reached a constant value. An example of the raw data used to generate the results in Table I is shown in Figure 1. The equilibration could be followed for long reaction times (to ~20 s) ensuring essentially complete thermalization. At the reactant pressures in this study equilibrium was usually established within ~3 s, and ion loss from the cell was negligible during this time. Ejection of each parent ion prior to equilibrium was used to show that equilibrium constants obtained do not depend on direction of approach to equilibrium.

For the series of $M(hfac)_3$ complexes, an order of increasing values of $-\Delta G_a°$ for eq 1 at 350 K was found by bracketing the complexes against each other. By the admission of roughly equal pressures of various combinations of two $M(hfac)_3$ complexes into the FTICR and the observation of which of the two parent negative ions predominated after a charge-transfer period, the relative order for the series of complexes was determined.

The ion gauge on the mass spectrometer was calibrated for each compound studied by using an external MKS baratron capacitance manometer in the pressure range $\sim 10^{-5}$ Torr. Special pressure calibration procedures developed for the FTICR systems were used that ensure uniform reactant gas pressure throughout the system by adjusting the relative pumping rates of the two diffusion pumps connected to the high-vacuum chamber.

Gas-Phase Spectrophotometry. Gas-phase visible spectra of the $M(hfac)_3$ complexes were determined by using a specially designed sample cell with 10 cm path length and fitted with heated quartz windows and a separately heated cell body. Crystals of a $M(hfac)_3$ complex were added to the cell, which was then evacuated and positioned in the cell compartment of an IBM UV/visible 9430 spectrophotometer. The cell was gradually heated to about 80 °C to produce a practical concentration of vapor.

Results

Consistency of Electron Attachment Energy Determinations. Although the lower operating pressures of ICR and FTICR compared to PHPMS enable low-volatility coordination compounds to be studied,[32] this can also introduce greater uncertainty in the measurement of reactant pressures. To check the consistency of our results with previous determinations, we measured K_{rxn} for the reaction A = 1,4-dicyanobenzene and B = 3-fluoronitrobenzene in eq 2. For this reaction at 423 K Kebarle and Chowdhury[25] found $\Delta G_{rxn}° = -3.2$ kcal mol^{-1} and $\Delta S_{rxn}° = 2.5$ cal deg^{-1} mol^{-1}, giving a value of $\Delta H_{rxn}°$ of -2.1 kcal mol^{-1}. In the FTICR at 350 K we obtained $\Delta G_{rxn}° = -2.8$ kcal mol^{-1}, which together with the previously determined entropy change

(27) Heinis, T.; Chowdhury, S.; Scott, S. L.; Kebarle, P. *J. Am. Chem. Soc.* **1988**, *110*, 400.
(28) Paul, G.; Kebarle, P. *J. Am. Chem. Soc.* **1989**, *111*, 464.
(29) Cellota, R. J.; Bennett, R. A.; Hall, J. L. *J. Chem. Phys.* **1974**, *60*, 1740.
(30) Nimlos, M. R.; Ellison, G. B. *J. Phys. Chem.* **1986**, *90*, 2574.
(31) Recent reviews of the technique: (a) Buchanan, M. V.; Comisarow, M. B. In *Fourier Transform Mass Spectrometry*; Buchanan, M. V., Ed.; ACS Symposium Series 359; American Chemical Society: Washington, DC, 1987; pp 1–21. (b) Eyler, J. H.; Baykut, G. *Trends Anal. Chem.* **1986**, *5*, 44. (c) Marshall, A. G. *Acc. Chem. Res.* **1985**, *18*, 316.
(32) Sharpe, P.; Richardson, D. E. *Coord. Chem. Rev.* **1989**, *93*, 59.

gives $\Delta H_{rxn}° = -1.9$ kcal mol^{-1}. The discrepancy of 0.2 kcal mol^{-1} probably arises from the uncertain temperature of the neutral gas and error in measuring equilibrium constants that are close to the limit of detection ($0.01 < K_{rxn} < 100$) on our instrument. The value of $\Delta G_{rxn}°$ for this reaction therefore represents a value close to the upper limit of the range of values that may be confidently measured. The discrepancy can be considered an estimate of the expected error for free energies determined for equilibrium reactions, and we typically assign conservative uncertainties of 0.5 kcal mol^{-1} to values of $\Delta G_a°$ determined by equilibrium to account for experimental uncertainties, including temperature, pressure, and uncertainties in the assigned thermodynamic quantities for most of the reference compounds.

Tris(hexafluoroacetylacetonate) Complexes. The M(hfac)$_3$ complexes studied in this investigation were those of the first-row transition metals from Sc (d^0) to Co (d^6) and Ga (d^{10}). These complexes are particularly volatile and are easily admitted into the FTICR through leak valves on the inlet system. It has been shown previously[6,8] that for a series of first-row transition-metal M(hfac)$_3$ complexes that fragmentation following electron capture increases from left to right in the row. The same general trend was observed in the FTICR in this work. The major pathway to fragmentation was loss of a ligand ion, and this ion predominated in the mass spectra of the Fe and Co complexes immediately after electron capture. A few hundred milliseconds after the ionization, the parent ion was formed by charge transfer to the neutral complex from the fragment ions. After a suitable period of time, any remaining fragment ions were ejected from the cell.

By observation of charge-transfer reactions involving M(hfac)$_3$ complexes and organic reference compounds, it was found that few reference compounds had $-\Delta G_a°$ values as high as those of the complexes. The Fe, Co, and Mn complexes had electron affinities greater than any of the organic compounds so far reported. The reference compounds used and the observed reactions are shown in Figure 2. Values of $\Delta G_a°$ and $\Delta H_a°$ for the organics were taken from the literature.[23-28] In the instances where a charge-transfer equilibrium was observed between an organic reference compound and a metal complex, the value of $\Delta G_a°$ for the complex was obtained from the value of $\Delta G_{rxn}°$ given by the measured equilibrium constant and a value of $\Delta G_a°$ for the organic compound at the reaction temperature of 350 K (obtained for each organic compound from the tabulated values of $\Delta H_a°$ and ΔS_a). Although $\Delta G_a°$ values could not be experimentally measured for Fe(fhac)$_3$, Co(hfac)$_3$, and Mn(hfac)$_3$, estimates were obtained by noting that the order of the $\Delta G_a°$ values runs parallel for both series of complexes. The difference in $\Delta G_a°$ values between V(acac)$_3$ and V(hfac)$_3$ was determined to be ~50 kcal mol^{-1} from the results of two separate equilibrium reactions, and the bracketed $\Delta G_a°$ values for Cr(acac)$_3$ and Cr(hfac)$_3$ were also separated by 50 ± 5 kcal mol^{-1}. Assuming a constant difference of 50 kcal mol^{-1} between the M(acac)$_3$ and M(hfac)$_3$ complexes of the other metals in the series, estimates could be made for the M(hfac)$_3$ complexes (M = Fe, Co, Mn), since those for the M(acac)$_3$ complexes of the same metals were measurable. $\Delta G_a°$ values for all the complexes are reported in Table I.

The substance with the highest accurately known electron affinity is the chlorine atom, and Cl$^-$(g) ion was included in the study of charge-transfer reactions with the metal complexes. Electron capture by a background pressure of Fe(hfac)$_3$ with a small partial pressure of benzyl chloride produced Cl$^-$ in addition to the ions formed from the metal complex. It was found that when all ions except chloride were ejected from the cell and its subsequent reaction with Fe(hfac)$_3$ was followed, chloride ion regenerated Fe(hfac)$_3^-$ by charge transfer, indicating that the electron affinity of Fe(hfac)$_3$ > 83.4 kcal mol^{-1},[33] in accord with the value estimated above.

Charge transfer occurred from tetrachlorobenzoquinone (Cl$_4$BQ)$^-$ to Cr(hfac)$_3$, but an equilibrium reaction was not observed in the reaction with Sc(hfac)$_3$, as the reaction was hampered by rapid formation of adduct ions, [Sc(hfac)$_3$·Cl$_4$BQ]$^-$, and [Sc(hfac)$_3$]$_2^-$.

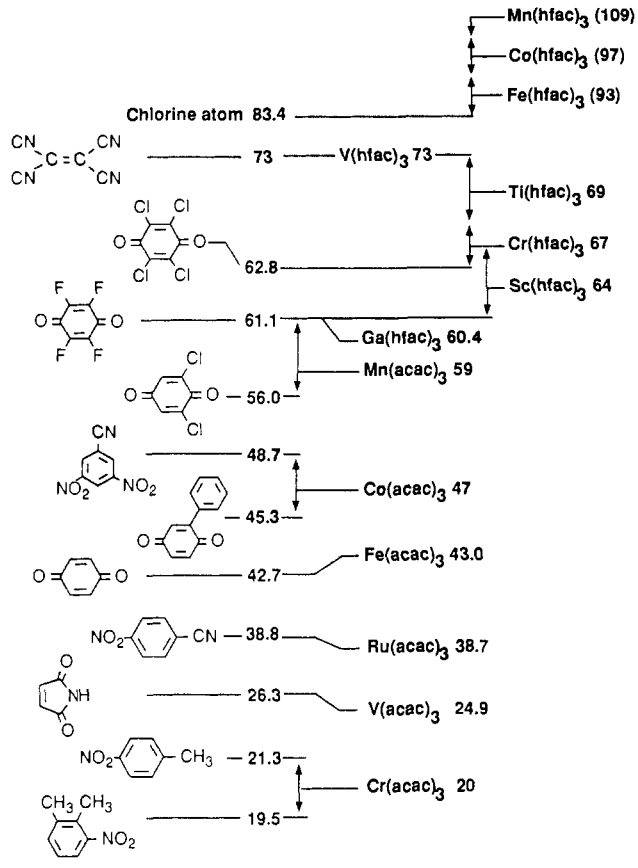

Figure 2. Free energies of electron attachment ($-\Delta G_a°$ values given in kcal mol^{-1}) to M(acac)$_3$ and M(hfac)$_3$ complexes at ~350 K and reference compounds used. A continuous line linking an organic compound and a metal complex indicates the value for the complex was obtained from a measured equilibrium constant (eq 2). Arrows indicate the compounds of greater and lower $\Delta G_a°$ values used to bracket the value for the metal complex (Scheme I). Values for M(hfac)$_3$ with M = Mn, Co, and Fe are estimates (see text).

Tris(acetylacetonate) Complexes. M(acac)$_3$ complexes were studied for the series of metals Sc–Co, Ga, and Ru. Ru(acac)$_3$ was included because it has a reversible reduction potential in water and was a suitable complex to include in the thermochemical cycle described in the companion article.[17] It has been previously noted that the cross section for electron capture by first-row transition-metal M(acac)$_3$ complexes is much lower than that for the corresponding M(hfac)$_3$ analogues.[7] Indeed, Cr(hfac)$_3$ was shown to have an electron capture cross section some 5000 times greater than that for Cr(acac)$_3$.[7] This was attributed to the six electron-withdrawing CF$_3$ ring substituents in the former. The same general effect was observed in this report for the complexes of the metals Cr to Co. The only ion produced from ionization of the neutral gas with the electron beam was ligand anion, but unlike the M(hfac)$_3$ complexes, the ligand ion did not charge transfer to the neutral complex to form the parent ion. Parent negative ions of these complexes could only be obtained in reasonable yields following chemical ionization by an organic compound of lower electron affinity. In performing experiments with these compounds, therefore, it was necessary to eject relatively large amounts of ligand anion from the cell. The Ti and V complexes produced no detectable fragment ions and had large cross sections, in accord with the trends in stability of the ions noted above.

The difference in the electron-withdrawing effect between CF$_3$ and CH$_3$ in the two series of complexes was also observed to markedly reduce the electron affinity of the M(acac)$_3$ series relative to the M(hfac)$_3$ series, and the values of $\Delta G_a°$ fall well

(33) McDermid, I. S.; Webster, C. R. *J. Phys.* **1983**, *44*, C7-461.
(34) Endo, A.; Watanabe, M.; Hayashi, S. *Bull. Chem. Soc. Jpn.* **1978**, *51*, 800.

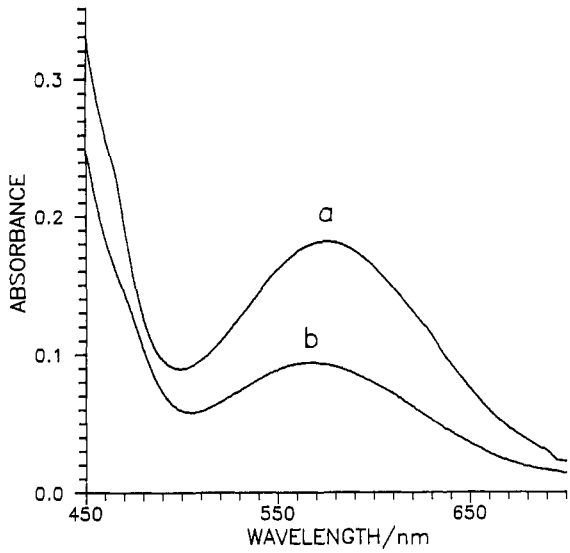

Figure 3. Comparison of absorbance bands for the $^4A_{2g}$–$^4T_{2g}$ transition in $Cr(hfac)_3$ in the gas phase at ~350 K (a) and in ethanol at room temperature (b).

within the range of those of the organic compounds in the reported electron-transfer free energy ladder, which extends from approximately −10 to −75 kcal mol^{-1}.[16] This enabled bracketing and equilibrium reactions in Scheme I and eq 2 to be followed for the entire series of $M(acac)_3$ complexes. The results for the values of $\Delta G_a°$ for the $M(acac)_3$ series obtained in this way are given in Figure 2 and Table I. The $Cr(acac)_3$ ion, although initially produced in the FTICR cell, was unstable and underwent rapid loss of ligand ion at a rate that increased with the total pressure of the system, indicating a collisionally induced dissociation. The instability of $Cr(acac)_3^-$ has been observed previously.[3] Bracketing this compound through charge-transfer reactions was therefore hampered by competitive ligand loss, producing a greater uncertainty in the result. Parent negative ions could not be made for the Sc and Ga complexes. Assuming a parallel trend with ~50 kcal mol^{-1} separation between the $M(hfac)_3$ series and $M(acac)_3$ series, then electron attachment to the Sc and Ga complexes would be expected to be only modestly exoergic, and experimentally, no parent ions were observed.

A value of $\Delta G_a°$ for the $Ti(acac)_3$ complex could not be obtained. In contrast to all the other complexes studied, $Ti(acac)_3$ or its anion did not undergo detectable electron exchange with most reference compounds prior to essentially complete ion loss from the FTICR ion trap, even with relatively high pressures of neutral gas. Exothermic charge-transfer reactions involving $Ti(acac)_3$ with various organic reactants were too slow to follow ($k_{rxn}/k_{collsn} \leq 10^{-4}$) over the range of up to 1 eV of driving force. The cause of this unexpectedly slow gas-phase charge transfer is not known and would not have been predicted for a d^1/d^2 redox process.

Charge-transfer equilibria were observed for the V (Figure 1) and Fe complexes, and results for Cr, Mn, and Co were obtained by the bracketing technique outlined in Scheme I.

Gas-Phase Visible Absorbance Spectra. A comparison of the visible spectra of $Cr(hfac)_3$ in the gas phase and in ethanol solution is shown in Figure 3. The band maxima in the region of the metal d–d transitions differ by ~7 nm. Absolute intensity measurements were not measured for the gas-phase complex.

Discussion

Free Energies of Electron Capture and Electron Affinities. Under the stationary electron (ion) convention,[35] the relationship between ΔG_a and EA for the general reaction $A + e = A^-$ is given in eq 3. The expression contains the heat capacities of a neutral

$$EA = -\Delta G_a - T\Delta S_a + \int_0^T Cp(A^-)\,dT - \int_0^T Cp(A)\,dT \quad (3)$$

species (A) and its anion (A^-) integrated from absolute zero to the reaction temperature. Appropriate spectroscopic data, although scarce, is available for negative ions of some organic and inorganic compounds to enable the difference between the integral terms to be evaluated by the methods of statistical thermodynamics.[36,37] When the acceptor orbital is nonbonding or a delocalized π^* in an aromatic molecule, the differences in structure and bonding between a neutral and its anion are small, and the integral terms can usually be neglected. Statistical thermodynamics also predicts only small values for ΔS_a for such cases. This prediction has been confirmed experimentally from the large number of studies of the temperature dependencies of charge-transfer equilibria involving organic compounds. Thus, experimental values of $-\Delta G_a°$ are therefore typically within ~2 kcal mol^{-1} of the EA value for these types of organic molecules.[24]

In contrast to the organic acceptors described above, statistical thermodynamics predicts larger differences between the values of $-\Delta G_a°$ and EA for electron capture by certain coordination compounds.[37] Shifts in the metal–ligand vibrational frequencies often found when the metal oxidation state changes can be shown to contribute markedly to entropy changes.[37] Changes in electronic degeneracy of the complex ground states following reduction can also lead to significant electronic entropy changes. Vibrational contributions to differences in integrated heat capacities may also become significant. Thus, for complexes in this study, couples that involve changes in occupancies of antibonding orbitals may have substantial values of ΔS_a for eq 1 (i.e., Cr(III)/Cr(II), low-spin Co(III)/high-spin Co(II), Mn(III)/Mn(II)), and in those cases, the observed $-\Delta G_a°$ values may differ from the true EA significantly (>2 kcal mol^{-1}).[38]

The highest lying molecular orbitals in transition-metal acetylacetonate complexes have been shown by photoelectron spectroscopy[18] and Xα calculations[39] to be metal based. Magnetic susceptibility studies[40–42] have shown the series of complexes in this study to be high spin, except for those of cobalt(III), which have a low-spin d^6 configuration. Comparison of gas-phase and solution-phase UV–visible spectra of hexafluoroacetylacetonate compounds show only minor shifts in absorbance maxima (for example, Figure 3), and the complexes are expected to have the same electronic configurations in the gas phase. The structural similarity of $Cr(hfac)_3$ between the solid and gas phases has also been noted.[43] Electron capture is therefore expected to cause a formal reduction at the metal center, except for closed-shell $Ga(hfac)_3$ (d^{10}). For the complexes of Sc, Ti, V, Fe, and Ru, the captured electron enters a nonbonding (t_{2g} in the O_h point group) molecular orbital, and relatively small structural changes can be expected.[37] For the compounds of Cr and Mn, structural changes may be larger as the electron enters the metal-based σ^* set (e_g in O_h point group). This effect is expected to be greatest for the low-spin Co complexes, since a spin change from low-spin d^6 to high-spin d^7 occurs on reduction, placing two electrons in the e_g set.

Theoretical Analysis of Electron Affinity Trends. For a series of transition-metal ions in the same ligand environment, the

(35) (a) Lias, S. G., Bartmess, J. E., Liebman, J. F., Holmes, J. L., Levin, R. D., Mallard, W. G., Eds. *Gas-Phase Ion and Neutral Thermochemistry*; American Institute of Physics: New York, 1988. (b) Sharpe, P.; Richardson, D. E. Submitted for publication.

(36) A discussion of the methods of calculation with examples can be found in the following references: (a) Lias, S. G.; Ausloos, P. *J. Am. Chem. Soc.* **1978**, *100*, 6027. (b) Loewenschuss, A.; Marcus, Y. *Chem. Rev.* **1984**, *84* (2), 89.

(37) Sharpe, P.; Richardson, D. E. Manuscript in preparation.

(38) Temperature-dependent equilibrium studies in the FTICR method have not been well developed. We are currently exploring experimental approaches to obtaining reliable temperature dependencies for equilibrium studies.

(39) Lussier, L. S.; Sandorfy, C.; Goursot, A.; Penigault, E.; Weber, J. *J. Phys. Chem.* **1984**, *88*, 5492.

(40) Jarret, H. S. *J. Chem. Phys.* **1957**, *27*, 1298.

(41) Guha, B. C. *Proc. R. Soc. London* **1951**, *A206*, 353.

(42) Whipple, R. O.; West, R.; Emerson, K. *Inorg. Chem.* **1965**, *4* (1), 130.

(43) Thomas, B. G.; Morris, M. L.; Hilderbrandt, R. L. *Inorg. Chem.* **1978**, *17* (10), 2901.

Table II. Energies of Electronic States for d^q Free Ions and Octahedral ML_6 Complexes (q = 1–7)[a]

	free ion		ML_6 complex	
d^q	term	energy	term	energy
d^1	^2D	$-E_0$	$^2T_{2g}$	$-\epsilon - 4Dq$
d^2	^3F	$-2E_0 + A - 8B$	$^3T_{1g}$	$-2\epsilon + A - 0.5B - 3Dq - 0.5(225B^2 + 180B(Dq) + 100Dq^2)^{1/2}$
d^3	^4F	$-3E_0 + 3A - 15B$	$^4A_{2g}$	$-3\epsilon + 3A - 15B - 12Dq$
d^4	^5D	$-4E_0 + 6A - 21B$	^2E_g	$-4\epsilon + 6A - 21B - 6Dq$
d^5	^6S	$-5E_0 + 10A - 35B$	$^6A_{1g}$	$-5\epsilon + 10A - 35B$
d^6	^1I	$-6E_0 + 15A - 29B + 13C$	$^1A_{1g}$	$-6\epsilon + 15A - 24Dq - 30B + 15C - (12B^2/Dq)$
d^6	^5D	$-6E_0 + 15A - 35B + 7C$	$^5T_{2g}$	$-6\epsilon + 15A - 35B + 7C - 4Dq$
d^7	^4F	$-7E_0 + 21A - 43B + 14C$	$^4T_{1g}$	$-7\epsilon + 21A - 35.5B + 14C - 3Dq - 0.5(225B^2 + 180B(Dq) + 100Dq^2)^{1/2}$

[a] The reference energies (zero of potential energy) for this table are the energies of the core ions or complex ions with all d electrons removed. E_0 and ϵ represent the effective one-electron binding energy to the core ion and complex ion, respectively. Ground-state terms are given for all free ions, but the excited ^1I state for d^6 is also included, since it is the parent term for the low-spin $^1A_{1g}$ state in d^6 complexes. Expressions for term energies are adapted from refs 51 and 56. Note that ϵ contains the energy perturbation due to the spherical potential of the ligand field *and* the one-electron binding energies in the absence of a field.

variation of the free energy of electron attachment with electronic configuration could be modeled by using a variety of theoretical approaches. In the Slater–Condon–Shortley (SCS) model,[44,45] electron–electron interactions in the electronic structure of atoms and ions are typically related by the Racah parameters A, B, and C, the last two of which are adjustable parameters in the interpretation of atomic spectra. Ligand field theory is a perturbational extension of the SCS model to complexes.[46,47] The ligand field model is clearly a data reduction model for fitting spectroscopic band energies and is not competent to predict the changes in electron binding energies in going from a free ion to a complex (it is these binding energies that determine the *magnitude* of electron attachment energies for a complex). Instead, LFT has been used to predict relatively small energetic perturbations that accompany the splitting of the d levels in complexes and the effect of these perturbations on the thermodynamic properties of metal complexes.[1,46,48] A detailed molecular orbital treatment (for example, at the restricted Hartree–Fock SCF level[49]) presents a more complete view of electronic structure and has the additional advantage of predicting the changes in total energy quantities associated with processes such as electron attachment and bond dissociation. However, in this discussion we will apply the ligand field model to the process of electron attachment in an attempt to quantify the effect of electron–electron interactions and orbital splittings in the valence orbitals of complexes. The origins of the trends in electron attachment energies for free metal ions will be reviewed first, since the formation of complexes can be treated to a first approximation as a perturbation of the electronic structure of free ions.

Free Ions. The electron attachment energy (ΔE_a) of a free $M^{3+}(g)$ ion is equivalent to the negative of the third ionization potential (IP_3) of M(g), and the values are presented Figure 4 (triangles) for first-row transition elements.[50] Quantum expressions[51] for the energy of the ion ground states are given in Table II. The one-electron binding energies E_0 increase in going left to right in the series as a result of the increasing nuclear charge, and the general trend in IP_3 values is therefore an increase with higher atomic number. Electron repulsion and exchange interactions account for the deviations from a smooth trend as the atomic number increases. For example, the precipitous drop of 69.7 kcal/mol that occurs in $-\Delta E_a$ values from $Mn^{3+}(g)$ to $Fe^{3+}(g)$ can be explained by the maximizing of stabilizing exchange interactions for d^4 Mn^{3+} going to d^5 Mn^{2+}; the added electron in the Fe case enters an occupied orbital (increasing repulsions) without benefit of exchange stability (since its spin is opposite to that of the five other unpaired valence electrons).

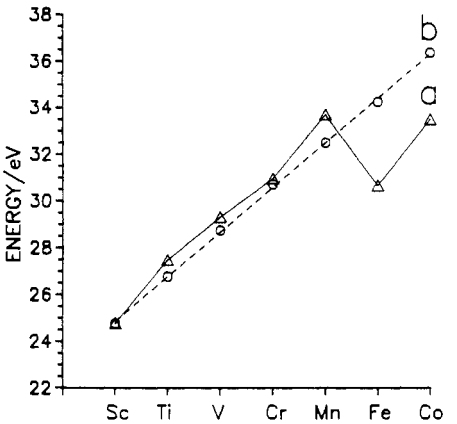

Figure 4. Energies for electron attachment to $M^{3+}(g)$ metal ions (triangles) and the values obtained by subtracting Racah B and C terms obtained from fits to the line spectra of the ions (circles). Values of $-\Delta E_a$ are given and are equivalent to the ionization energy for $M^{2+}(g)$.

The theoretical expressions for electron attachment energies (ΔE_a) for the $M^{3+}(g)$ ions are readily derived from the energy expressions in Table II. For example, the value for $Fe^{3+}(g)$ is given by eq 4. The subscripts "5" and "6" in eq 4 refer to the d^5 and

$$-\Delta E_a(Fe^{3+}) = 30.64 \text{ eV} = E(d^5) - E(d^6) = (-5E_0 + 10A_5 - 35B_5) - (-6E_0 + 15A_6 - 35B_6 + 7C_6) = E_0 + (10A_5 - 15A_6) + (35B_6 - 35B_5) - 7C_6 \approx E_0 + (-62 \text{ eV}) + (-0.2 \text{ eV}) - (3.4 \text{ eV}) \quad (4)$$

$d^6(^5D)$ ions, respectively. The values of the A terms have been estimated by using Slater's rules[51] to construct approximate radial wave functions for the 3d electrons followed by calculation of the F_0 integral ($A = F_0 - (49C/35)$).[44,45,47] The B- and C-term values have been taken from the fits to line spectra of the ions.[51] From the values given in eq 4, the value of E_0 is estimated as 96 eV. The A terms (which primarily reflect the e^-/e^- repulsions arising from the radial part of the wave functions) clearly have a large affect on the final $-\Delta E_a$ value, but the trend in A contributions is a generally smooth increase with increasing atomic number.[51] The deviation for the $-\Delta E_a$ of $Fe^{3+}(g)$ to lower value from the smooth trend thus is traced in this model primarily to the repulsion integrals contained in the Racah parameter $7C_6$ in eq 4.

In Figure 4, the spectroscopic values of B and C are used to remove the contributions of those terms from the observed ΔE_a values for the first transition series $M^{3+}(g)$ ions, and the resulting points demonstrate the relatively linear change in the E_0 and A

(44) Slater, J. C. *Quantum Theory of Atomic Structure*; McGraw-Hill: New York, 1960; Vol. 1.
(45) Condon, E. U.; Shortley, G. H. *The Theory of Atomic Spectra*; Cambridge University Press: Cambridge, England, 1962.
(46) Figgis, G. N. *Introduction to Ligand Fields*; Wiley-Interscience: New York, 1966; pp 98.
(47) (a) Ballhausen, C. J. *Introduction to Ligand Field Theory*; McGraw-Hill: New York, 1962. (b) Schlafer, H. L.; Gliemann, G. *Basic Principles of Ligand Field Theory*; Wiley Interscience: New York, 1966. (c) Gerloch, M.; Harding, J. H.; Wooley, G. *Struct. Bonding* **1981**, *46*, 1.
(48) Burdett, J. K. *Molecular Shapes*; Wiley-Interscience: New York, 1980.
(49) Vanquickenborne, L. G.; Hendrickx, M.; Postelmans, D.; Hyla-Kryspin, I.; Pierloot, K. *Inorg. Chem.* **1988**, *27* (5), 900.
(50) Moore, C. E. *National Standard Reference Data Series 34*; U.S. Government Printing Office: Washington, DC, 1970.
(51) Griffith, J. S. *The Theory of Transition Metal Ions*; University Press: Cambridge, England, 1964.
(52) Slater, J. C. *Phys. Rev.* **1930**, *36*, 57.

Table III. Ligand Field Parameters for $M(acac)_3^{0/-}$ Complexes

M	g	k	$\Delta/10^3$ cm^{-1} [a]	B/cm^{-1} [b]	ΔLFSE/ kcal mol^{-1} [c]
Sc(II)	8[d]		8.4		
Sc(III)					−10
Ti(II)	10.6[e,f]	0.35[e,f]	11.1	190	
Ti(III)	20.3		21.3		−1
V(II)	12.3	0.08	12.9	640	
V(III)	18.6	0.3[e,g]	19.5	320	0.4
Cr(II)	14.1	0.1[d]	14.8	660	
Cr(III)	17.0	0.21	17.9	644[h]	36
Mn(II)	8.5	0.07	8.9	820	
Mn(III)	21	0.2[d]	22.1	660	38
Fe(II)	10.0	0.1[d]	10.5	840	
Fe(III)	14.0	0.24	14.7	536[h]	−12
Co(II)	9.3	0.24	9.8	480	
Co(III)	19.0	0.35	20.0	290	77

[a] $\Delta = f \cdot g$, with f(acac) = 1.05. [b] $B = h \cdot k$, with h(acac) = 2.1. [c] Difference in ligand field stabilization energies (strong-field limit) for the process $M(acac)_3 \rightarrow M(acac)_3^-$. A negative value implies that the electron attachment is favored by ΔLFSE. [d] Estimated by extrapolation (no useful spectroscopic information available). [e] Estimated from limited spectral data. [f] Hexachloro complex (ref 56, p 399). [g] Hexaaqua complex (ref 56, p 402). [h] References 54 and 55.

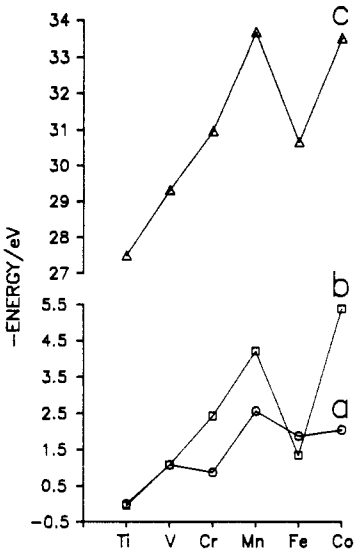

Figure 5. Observed free energies of electron attachment to $M(acac)_3(g)$ complexes (circles) and the values obtained by subtracting the appropriate ΔLFSE values in Table III (squares). Energies of electron attachment to $M^{3+}(g)$ ions are provided for comparison (triangles). Note that the value for $Ti(acac)_3$ is a lower limit for $-\Delta G_a$ (see text).

contributions as atomic number increases (dashed line). A similar analysis is given by Griffith.[51] The functional form of this line is given in eq 5 for a d^q ion. When the estimated A terms are

$$E = E_0 + (q(q-1)A_q)/2 - (q(q+1)A_{q+1})/2 \qquad (5)$$

included in the treatment, a second line is generated that gives the estimated value of E_0 as a function of the nuclear charge (not shown). The value of the SCS model in describing the energetics of electron attachment to free ions lies in the apparent success found in quantifying the energy contributions of e^-/e^- interactions through the use of parameters obtained by fitting the model to results of atomic spectroscopy.

Ligand Field Stabilization Approach. The concept of ligand field stabilization energy (LFSE) has been applied in the interpretation of electrode potentials for $[M(H_2O)_6]^{3+/2+}$(aq) and other couples,[1,46,53] and it is worthwhile initially to consider its application to the gas-phase data reported here. These rationales are based on the changes in LFSE that accompany the change in electron occupancy of the metal-based orbitals (i.e., $d^q + e^- \rightarrow d^{q+1}$). This approach represents the most elementary application of LFT to the thermodynamic problem, and a more detailed procedure analogous to that done for the free ions above is presented later. For purely high-spin redox couples, only the value of Δ ($=10Dq$) enters into the calculation of relevant LFSE values. When a spin change occurs (as for $Co(acac)_3 \rightarrow Co(acac)_3^-$), calculation of the pairing energy requires B and C values. The spectroscopic LFT parameters for the complexes of acac and hfac are not well-known due to the obscuring of many of the d–d bands by charge-transfer bands. However, Jorgensen f and h parameters can be derived for the ligands[54,55] and should provide sufficiently accurate estimates of LFT parameters for our purposes when combined with established g and k parameters[56] for the metals (Table III). It is also necessary at this level to assume an octahedral field, since the spectral details for the various complexes are not available to fit the LFT for the lower symmetry of these tris chelate complexes. Although the comparison in Figure 3 suggests that d–d bands are essentially unchanged from those in solution for gas-phase $M(acac)_3$ complexes, a possible criticism arises concerning the use of the Jorgensen parameters for the anionic M(II) complexes, for which little spectroscopic information is available. In the absence of data to the contrary, we will assume the M^{II} parameters apply.

The change in oxidation state for any couple is accompanied by a change in the amount of LFSE in the complex, and these values are summarized for the acac complexes in Table III. Note that the values of LFSE are based on the strong field expressions for these complexes,[58] and the value for the low-spin Co(III) complex includes the pairing energy correction $5B + 8C$. The observed $-\Delta G_a°$ values for the acac complexes are indicated by the circles on line a in Figure 5. The values of ΔLFSE are removed (squares on line b), and the resulting "corrected" points form a trend line very similar to that of the ΔE_a values for the free ions, shown by the points on line c. The ΔLFSE values can evidently be used qualitatively to rationalize the trends in $\Delta G_a°$ for these complexes, as found for the hexaaquo and other couples.[1,46,53] However, this approach ignores many of the essential details of the LF model and cannot be considered a rigorous application of the SCS model that forms the basis for the theory.

Detailed Ligand Field Treatment. In the context of the SCS model used above for free ions, ligation of the metal ions changes the ΔE_a and $\Delta G_a°$ values and trends significantly by lowering the values of E_0, splitting the degeneracy of the d orbitals, and changing the values of the Racah parameters A, B, and C. The interpretation of the markedly lower electron affinity for a given complex in comparison to the free ion is highly dependent on the bonding model used, but some general statements can be made. In the crystal field model, the effective d-orbital binding energy E_0 decreases upon ligation as a result of the spherical potential term of the field.[53c] In the molecular orbital model, the formation of delocalized orbitals leads to a lower "effective nuclear charge" for the valence orbitals, and the electron-acceptor LUMO has a much lower one-electron binding energy than the free metal ion orbital to which it correlates. Note also that the effective one-electron binding energy becomes strongly dependent on the metal oxidation state in a complex, since addition of an electron can lead to large nuclear and electronic relaxation (i.e., changes in bond

(53) (a) Dunn, T. M.; McClure, D. S.; Pearson, R. G. *Some Aspects of Crystal Field Theory*; Rice, S. A., Ed.; Harper and Row: New York, 1965; p 77. (b) Van Gaal, H. L. M.; Van der Linden, J. G. M. *Coord. Chem. Rev.* **1982**, *47*, 41. (c) Lintvedt, R. L.; Fenton, D. E. *Inorg. Chem.* **1980**, *19*, 571.
(54) Fatta, A. M.; Lindvedt, R. L. *Inorg. Chem.* **1971**, *10* (3), 478.
(55) Lindvedt, R. L.; Kernitsky, L. K. *Inorg. Chem.* **1970**, *9* (3), 491.
(56) Lever, A. P. B. *Inorganic Electronic Spectroscopy*, 2nd ed.; Elsevier: Amsterdam, 1984.
(57) Basolo, F.; Pearson, R. G. *Mechanisms of Inorganic Reactions*, 2nd ed.; Wiley: New York, 1967.
(58) March, J. *Advanced Organic Chemistry*, 3rd ed.; Wiley-Interscience: New York, 1985; pp 16–18, 237–250.

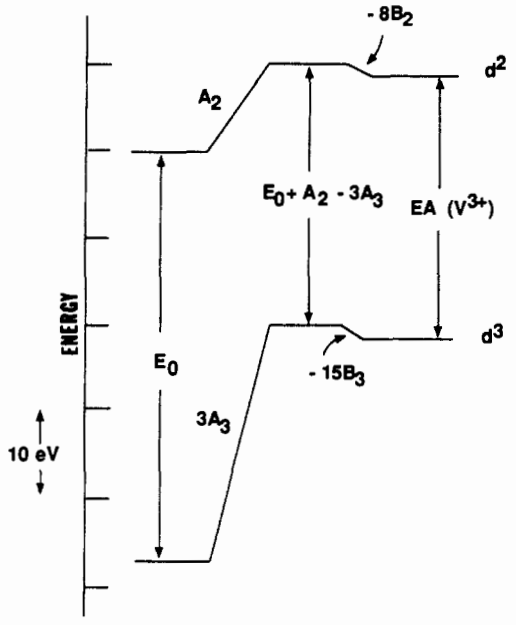

Figure 6. Quantitative illustration of the relative magnitudes of the one-electron binding energy (E_0) and Racah parameters that determine the energy difference between the ground-state terms for V^{+3} (d^2) and V^{+2} (d^3) ions (Table II).

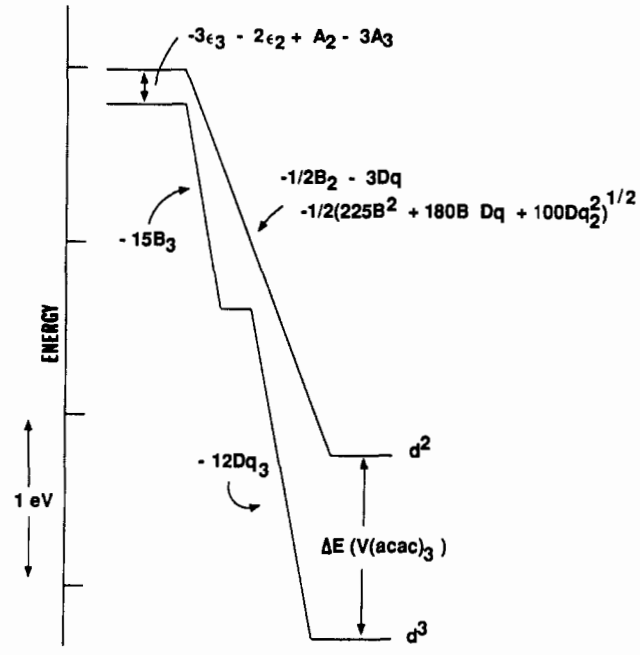

Figure 7. Quantitative illustration of the relative magnitudes of the one-electron binding energies to V(III) (ϵ_2) and V(II) (ϵ_3) $(acac)_3$ complexes and the energies from terms arising from the octahedral ligand field (Table II) that determine the energy of electron attachment to $V(acac)_3$.

lengths/angles and electron density distribution).

The sources of d-orbital splitting and changes in B and C from the free ion values have been studied intensively in coordination compounds.[46,47,51] Covalency in the bonding reduces e^-/e^- interactions in the primarily d valence orbitals, and thus the spectroscopically accessible B and C values are usually lowered from the free ion values (the nephelauxetic effect). The ligand field expressions for ground-state energies of the various d configurations are given in Table II along with the corresponding octahedral term symbols. For purposes of this discussion, all complexes are considered high spin with the exception of Co(III), so the weak field terms are generally given (except for d^6, for which both singlet and quintet terms are shown). The energy expressions include configuration interaction and are therefore general (they converge to the strong field values when $Dq \gg B$). In these energy expressions, the effective electron binding energy E_0 has been replaced for the complexes by ϵ to emphasize the large change in the one-electron binding energies from their free ion values and their oxidation state dependence.

We now ask whether the term energies in Table II can be used to interpret the trend in $\Delta G_a°$ values for the gas-phase complexes. One way to demonstrate this is to substitute available empirical parameters into the energy expressions and eliminate some of the contribution of valence level e^-/e^- interactions from the observed energies (exactly as was done above for the free metal ions). To illustrate the method used, electron attachment to d^2 V(III) will be considered in detail. A quantitative diagram of the relative term energies and their estimated components in the SCS scheme for the free $V^{3+}(g)$ ion is illustrated in Figure 6 (derived by an approach exactly analogous to that used for $Fe^{3+}(g)$ above). From the energy expressions in Table II, the ΔE_a of an octahedral $V(III)L_6$ complex is given by eq 6. In eq 6, the subscripts "2"

$$-\Delta E_a(V(III)L_6) = [-2\epsilon_2 + A_2 - 0.5B_2 - 3Dq_2 - 0.5(225B_2^2 + 180(Dq_2)B_2 + 100(Dq_2)^2)^{1/2}] - [-3\epsilon_3 + 3A_3 - 15B_3 - 12Dq_3] \quad (6)$$

and "3" refer to the parameters for the d^2 and d^3 complexes, respectively. Substituting the parameter values for the pseudooctahedral $V(acac)_3^{0/-}$ complexes from Table III yields eq 7.

$$-\Delta G_a°(V(acac)_3) \approx -\Delta E_a = 24.9 \text{ kcal mol}^{-1} = [3\epsilon_3 - 2\epsilon_2 + A_2 - 3A_3] + 22 \text{ kcal mol}^{-1} \quad (7)$$

The ΔE_a of $V(acac)_3$ is expected to be closely approximated by $\Delta G_a°$, since electron occupation of essentially nonbonding orbitals changes. Therefore, in eq 7 it will be assumed that $\Delta S_a°$ is small and $\Delta G_a° \approx \Delta E_a$. The value of the term in brackets in eq 7 is thus $\sim$3 kcal mol^{-1}, and the various contributions to the ΔE_a value for $V(acac)_3$ are summarized in Figure 7 (note the change in scale from Figure 6). The remaining unknown contributions are the one-electron binding energies ϵ and the Racah A parameters. The sources of the deviation of the $-\Delta E_a$ from the difference in the one electron binding energies ($3\epsilon_3 - 2\epsilon_2$) are the e^-/e^- interactions and the term interaction in the d^2 configuration ($^3T_{1g}(^3F)$/$^3T_{1g}(^3P)$). The strong field LFSE difference for the two oxidation states ($8Dq_2 - 12Dq_3$) is $\sim$0, so the energetic effects of e^-/e^- interactions dominate the divergence of ΔG_a for the complex from the smooth trend (i.e., the same effect found for the free V^{3+} ion but reduced in magnitude due to the nephelauxetic effect). The increase in $-\Delta E_a$ of 22 kcal mol^{-1}, which primarily results from the B terms, is a reflection of the exchange stability gained when an electron is added to the d^2 ion with all spins parallel (just as in the free ion). It is important to note that the values of the relevant parameters (A, B, and C) change significantly when the metal is complexed, and any quantitative model that uses the *observed* ΔE_a (ionization energy) values for the free metal ions as a starting point for explaining trends in quantities such as electrode potentials or $\Delta G_a°$ values for metal complexes is not a completely valid application of the SCS–ligand field model. Of course, this criticism applies to the LFSE treatment given above (Figure 5) for gas-phase ions and has been noted for LFSE treatments of electrode potential trends.[1]

The free energies of electron attachment to the acac complexes (corrected for electronic degeneracy contributions) are summarized in Figure 8, and the contributions to these values resulting from B and C terms have been applied as was done for the vanadium case above (assigning $C = 4B$). A trend line can be drawn through the points corresponding to the function of eq 8 (dashed line in

$$E = (q+1)\epsilon_{q+1} - q\epsilon_q + (q(q-1)A_q)/2 - (q(q+1)A_{q+1})/2 \quad (8)$$

Figure 8). Unlike the result for the free ions (Figure 4), the corrected points do not fall near the best fit line, and only a general upward trend can be discerned. The quantitative interpretation of the data provided by the detailed SCS–LFT model is not particularly superior to the simple LFSE approach (Figure 5).

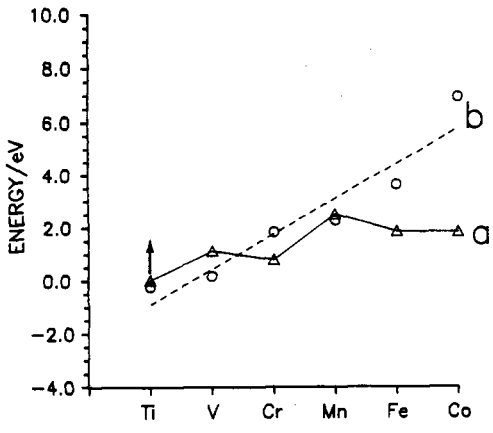

Figure 8. Plot of experimentally derived $-\Delta G_a°$ values for $M(acac)_3$ complexes (triangles) and the values obtained from them by subtracting the contribution to the energy of electron attachment due to e^-/e^- interactions derived from the detailed ligand field analysis (circles).

The model used here to discuss electron attachment to metal complexes is obviously inadequate to deal with the subtle interplays of e^-/e^- interactions, relaxation, and covalency that ultimately determine EA values. Of course, a poor "fit" to the data could arise if the LF parameters (Table III) are in gross error. However the Jorgensen *fg/hk* model is known to yield good predictions for Δ values,[56] and reasonable variations in *B* and *C* values have little effect on the interpretations here. It is noteworthy that the inadequate fit by the LFSE method is apparently *not* a result of a failure to include the effect of ligation on e^-/e^- interaction energies but is simply an illustration of the inherent limitations of the LF model in quantitative interpretation of thermochemical data.

It is clear that the most obvious general feature of the $\Delta G_a°$ trend (i.e., the reduction in the *range* of electron attachment energies for the complexes compared to the free ions) is explained by the approaches above. Both the LFSE approach and the full LFT treatment predict that the electron affinity for Cr(III), Mn(III), and especially Co(III) complexes will be reduced significantly by effects arising from the splitting in the primarily d valence orbitals. As a result the $\Delta G_a°$ values for the Ti–Co acac complexes cover a range of ~2 eV, while the same metals as free ions cover a range of ~7.5 eV (Figure 4). Note that when the $\Delta G_a°$ values are "corrected" for the effects of d-orbital splitting and part of the e^-/e^- repulsions, the range of the line for eq 8 (Figure 8) for the complexes from Ti–Co covers ~7 eV, while the analogous range (eq 5) for the free metal ions Ti^{3+}–Co^{3+} is comparable (~7.5 eV, dashed line in Figure 4). Thus, the overall trend in electron affinities for these complexes is crudely explained by the general trend for the free metal ions modified by the effects of the ligand field. Similar observations have been made for electrode potential trends of transition-metal complexes.[1,53]

The magnitudes of the influence of the LFSE on electron affinity values for metal complexes deserve some further comment. As generally applied to relative energies of possible kinetic intermediates[57] or ground-state structures,[48] LFSE values are normally thought of as small in relation to bond energies but nevertheless influential. In the case of gain or loss of an electron from a complex, however, the magnitude of the LFSE effect can be quite large (Table III). For example, for Co(III)/Co(II) examples here, the LFSE contribution on $\Delta G_a°$ is ~3 eV, which is comparable in magnitude to bond energies and the $\Delta G_a°$ values.

The $-\Delta G_a°$ values for the hfac complexes are ~50 kcal/mol higher than those of the acac complexes with the same metals. Since the Δ, *B*, and *C* values for the hfac complexes are not much different from those of the acac complexes,[54,55] the source of the higher electron affinities within the context of our model must be in the terms contained in eq 8. Fluorination of acac at the methyl substituents introduces a strong $-I$ field effect[58] at the periphery of the complex, and the reduced (anionic) complex is stabilized significantly relative to the oxidized (neutral) form.

Conclusions. The gas-phase data reported here provide a direct measure of the intrinsic redox properties of coordination complexes in the absence of solvation. The first extensive survey of adiabatic electron attachment energies for transition-metal coordination complexes in the gas phase has revealed several fundamental features of the thermodynamics of such processes. The trends in $\Delta G_a°$ values for the acac and hfac complexes closely parallel the trends in electrode potentials for the hexaaquo complexes in aqueous solution. The change in the trends in electron attachment energies for complexes in comparison to the corresponding free ions can be qualitatively explained through consideration of the effects of ligand field splitting of the primarily metal d valence orbitals. In particular, the much reduced range of values for $\Delta G_a°$ for M = Ti–Co (~2 eV) in comparison to the free ions (~7 eV) results primarily from lower ligand field stabilization of the reduced forms of the $M(acac)_3^-$ complexes for M = Cr, Mn, and Co relative to the $M(acac)_3$. An attempt to estimate these effects quantitatively via ligand field theory demonstrates the limitations of that model. The simplistic ligand field stabilization energy analysis of the trends apparently provides a useful qualitative interpretation of the data. A more rigorous application of LFT that accounts for configuration interaction and reduction in the values of the Racah parameters due to covalency produces a less than satisfactory quantitative interpretation of the experimental observations. The magnitudes of the $-\Delta G_a°$ values for the hfac complexes are ~50 kcal mol^{-1} higher than those for the corresponding acac complexes.

In general, it appears that quantitative LFT analysis of trends in transition-metal complex redox energetics here will be less than completely successful for several reasons. The LFT is a data reduction model for electronic spectroscopy and does not model only the ground electronic state of the complex. The relationship between spectroscopic model parameters and ground-state thermochemistry is not well defined, since the parameters typically are temperature dependent and are related to the characteristics of both ground-state and excited-state potential surfaces. Furthermore, the proper thermodynamic quantity (free energy or enthalpy) to be evaluated by a ligand field model is not rigorously defined. Effects of Jahn–Teller distortions on the energetics were not included but can be thermochemically important. In these types of couples, both oxidized and reduced molecules usually have unfilled valence configurations, so inadequacies in the electronic model for both species can contribute to poor fits to thermodynamic data. More detailed quantum models are obviously required to quantify the subtle energetic features of electron attachment to such large polyatomic species. Since solvation generally contributes significantly to the thermodynamics of redox processes, this type of adiabatic gas-phase data is more suitable than solution data for detailed theoretical analysis of redox thermochemistry via more sophisticated quantum models.

Acknowledgment. This work was supported by a grant from the National Science Foundation (CHE8700765). We are grateful for helpful discussions with C. Schaffer, M. Zerner, and D. Baker.